いたが[5]，本研究では，そのような傾向は認められなかった．これはTi表面をアルカリ溶液した効果によるものと考えられる[8,9]．

引張試験片から得られたHAコーティングのXRDによる生成相の同定結果から，オートクレーブ処理時間12時間以上の試料については，未反応物質や不純物の存在は認められなかった．これは以前に我々が報告した傾向と同様である[5]．以上の結果より，今回新たに開発したHAコーティング方法においても，以前に我々が報告した水熱ホットプレス法によるHA/Ti接合体と同様のHA生成プロセスを経ているものと考えられる．

4.結言

本研究により，水熱ホットプレス法の原理を応用した新たなHAコーティング法が開発された．このHAコーティングは容易にはく離するものではなく，HA/Ti界面はHAコーティング自体と同等ないしそれ以上のはく離強度を有している．また135℃もの低温プロセスで作製されるHAコーティングは，従来の作製方法で懸念されているHAの熱分解がなく，純度の高いHAコーティングを作製し得る方法であることが示された．

5.謝辞

本研究の一部は厚生労働省科学研究費補助金萌芽的研究先端医療技術推進事業(H14-ナノ-021)の助成によるものである．関係者各位に謝意を表する．

6.参考文献

1) 青木秀希：驚異の生体物質アパタイト，第1版，医歯薬出版 (1999).
2) 柳澤和道：水熱ホットプレス法，水熱科学ハンドブック（水熱科学ハンドブック編集委員会），1版，技報堂出版，(1997).
3) T. Onoki, K. Hosoi and T. Hashida : *Proc. Joint 6th ISHR & 4th ICSTR*, Japan, 549 (2000).
4) 小野木伯薫，細井和幸，橋田俊之 ： 日本生体電気刺激研究会誌(JJBERS)，**17**, 21 (2003).
5) 小野木伯薫，田中雅明，細井和幸，橋田俊之：2003年度傾斜機能材料論文集（FGM2003 in Sapporo)，1 (2004).
6) K. Hosoi, T. Hashida, H. Takahashi, *et al.* : *J. Am. Ceram. Soc.*, **79**, 771 (1996).
7) T. Matsuno and M. Koishi : Shikizai, 65, 238 (1992).
8) T. Onoki, K. Hosoi and T. Hashida : *Proc. 5th ICSTR*, USA, 250 (2002).
9) T. Onoki, K. Hosoi and T. Hashida : *Key Engineering Materials*, **240-242**, 571(2003) .

Available online at www.sciencedirect.com
SCIENCE DIRECT®
Scripta Materialia 52 (2005) 767–770
Scripta MATERIALIA
www.actamat-journals.com

New technique for bonding hydroxyapatite ceramics and titanium by the hydrothermal hot-pressing method

Takamasa Onoki [a,*], Kazuyuki Hosoi [b], Toshiyuki Hashida [a]

[a] *Fracture and Reliability Research Institute, Graduate School of Engineering, Tohoku University, Aoba 01, Aramaki, Aoba-ku, Sendai 980-8579, Japan*
[b] *Shiraishi Kogyo Kaisha Limited, 4-78 Motohama-cho, Amagasaki-shi 660-0085, Japan*

Received 31 May 2004; received in revised form 18 November 2004; accepted 7 December 2004

Abstract

Solidification of hydroxyapatite (HA:$Ca_{10}(PO_4)_6(OH)_2$) and its bonding with titanium (Ti) was achieved simultaneously by using the hydrothermal hot-pressing method at temperatures as low as 150 °C with no special surface treatment of Ti. A mixture of calcium hydrogen phosphate dihydrate and calcium hydroxide was used as the starting powder material for solidifying HA. Three-point bending tests were conducted to obtain an estimate of the fracture toughness for the HA/Ti interface as well as for the HA ceramics only. The fracture toughness tests showed that the induced crack from the pre-crack tip deviated from the HA/Ti interface and propagated into the HA. The fracture toughness determined on the bonded HA/Ti specimen was close to that of the HA ceramics only (~0.30 $MPa\,m^{1/2}$).

Keywords: Titanium; Hydroxyapatite; Hydrothermal; Bonding; Toughness

1. Introduction

Titanium (Ti) and its alloys are widely used as orthopedic and dental implant materials because of their high mechanical strength, low modulus and good corrosion resistance [1]. Traditionally, Ti and its alloys have been reported to be bioinert. When embedded in the human body, a fibrous tissue encapsulates the implant isolating it from the surrounding bone forms.

Some bioactive ceramics such as HA, bioglass and glass ceramics can directly bond to living bone when used as bone replacement materials [2–4]. In the traditional method for solidifying HA, HA powder is sintered at high temperatures over 1000 °C [5]. The mechanical properties of bulk HA only allow applications for small non-loaded structures [6]. The possibility of depositing it in films has permitted the exploitation of its bioactive properties in structural prostheses such as teeth roots, and in hip, knee and shoulder joint replacement. Therefore, HA is also used as a coating material for the surfaces of such prostheses in order to prepare bioactive layers on titanium and its alloys [7]. The HA surface improves the fixation of implants by the growth of bone into the coating, forming a mechanical interlock. A plasma spraying technique has been frequently employed for the coating process of HA [8,9]. However, this high temperature method results in some significant problems, such as poor coating–substrate adherence [10], and lack of uniformity of the coating in terms of morphology and crystallinity [11,12], which affect the long-term performance and the lifetime of the implants. In spite of various investigations being carried out, the coatings produced can suffer from at least one of the following problems: lack of coating adherence to the substrate, poor structural integrity and non-stoichiometric composition [13].

* Corresponding author. Tel.: +81 222 177 524; fax: +81 222 174 311.
E-mail address: onoki@rift.mech.tohoku.ac.jp (T. Onoki).

1359-6462/$ - see front matter © 2004 Acta Materialia Inc. Published by Elsevier Ltd. All rights reserved.
doi:10.1016/j.scriptamat.2004.12.011

Recently, it has been reported that surface modifications for forming bonelike apatite can induce high bioactivity of bioinert materials in simulated body fluid (SBF) [14]. In our previous research, therefore, the bonding of HA ceramics and Ti alloys (Ti–15Mo–5Zr–3Al and Ti–6Al–2Nb–1Ta) was achieved by the hydrothermal hot-pressing (HHP) method through the surface modification of Ti alloys with NaOH solution [15].

The HHP method is a processing route which makes production a ceramic body at relatively low temperatures possible [16]. The compression of samples under hydrothermal conditions accelerates densification of inorganic materials. It is known that the water of crystallization in calcium hydrogen phosphate dihydrate ($CaHPO_4 \cdot 2H_2O$; DCPD) is slowly lost below 100 °C [17]. If the released water can be utilized as a reaction solvent during the HHP treatment, it is to be expected that the joining of HA to metal can be achieved simultaneously under hydrothermal condition, in addition to the synthesis and solidification of HA through chemical reaction as follows [18]:

$$6CaHPO_4 \cdot 2H_2O + 4Ca(OH)_2 \rightarrow Ca_{10}(PO_4)_6(OH)_2 + 18H_2O \quad (1)$$

In the above mentioned previous study [15], however, the successful bonding to HA ceramics required the surface modification of Ti alloys using NaOH solution. The surface of Ti alloys needed to be treated with the NaOH solution before the bonding to HA ceramics. This paper demonstrates that bonding HA ceramics and pure Ti can be achieved by using the HHP method without special surface modifications of Ti.

2. Experimental procedure

A commercially available pure Ti rod (99.5%; Nilaco, Japan), 20 mm in diameter, was used in this experiment. The Ti rod was cut into disks with a thickness of 10 mm. The disks were cleaned in deionized water and acetone by using an ultrasonic cleaner. The Ti surfaces were finished using 1500# emery paper. After the surface finish with emery paper, the titanium disks were washed again with deionized water, and then dried in air.

DCPD used as the starting powder was prepared by mixing 1.0 M calcium nitrate solution (99.0%; $Ca(NO_3)_2 \cdot 4H_2O$, Kanto Chemical, Japan) and 1.0 M diammonium hydrogen phosphate solution (98.5%; $(NH_4)_2HPO_4$; Kanto Chemical, Japan). The mixing was carried out at a room temperature (at ≈20 °C). In order to control the pH value, acetic acid and ammonia solution were added. The precipitate from the mixture was filtered and washed with deionized water and acetone. The washed filter cake was oven-dried at 50 °C for 24 h, and then the dried cake was ground to a powder.

The synthetic DCPD and calcium hydroxide (95.0%; $Ca(OH)_2$; Kanto Chemical, Japan) were mixed in a mortar for 90 min with a Ca/P ratio of 1.67. The powder mixture and Ti disks were placed into the middle of an autoclave simultaneously, as shown in Fig. 1. The steel autoclave has pistons within a cylindrical structure with an inside diameter of 20 mm. The pistons enable the hydrothermal solution squeezed from the sample to escape, and this regulates the appropriate hydrothermal conditions in the sample. Polytetrafluoroethylene (PTFE) is packed between a cast rod and a push rod. The PTFE was used to prevent leakage of the hydrothermal solutions.

A pressure of 40 MPa was initially applied to the sample through the push rods from the top and the bottom at room temperature. After the initial loading the autoclave was heated upto 150 °C at a heating rate of 10 °C/min, and then the temperature was kept constant for 2 h. The autoclave was heated with a sheath-type heater. The axial pressure was kept at 40 MPa during the HHP treatment. After the treatment, the autoclave was naturally cooled to room temperature, and the sample removed from the autoclave.

The shrinkage behavior of the sample during the HHP treatment was monitored by measuring the relative movement between the two pistons using a displacement gage. The displacement data were used to determine the volume ratio V of the sample, defined as follows:

$$V = (h_i - \Delta h)/h_i \times 100 \quad (2)$$

where h_i is the initial sample height, and Δh is the relative displacement during the heating process.

Three-point bending tests were conducted to obtain an estimate of the fracture toughness for the HA/Ti interface as well as for the HA ceramics made by the

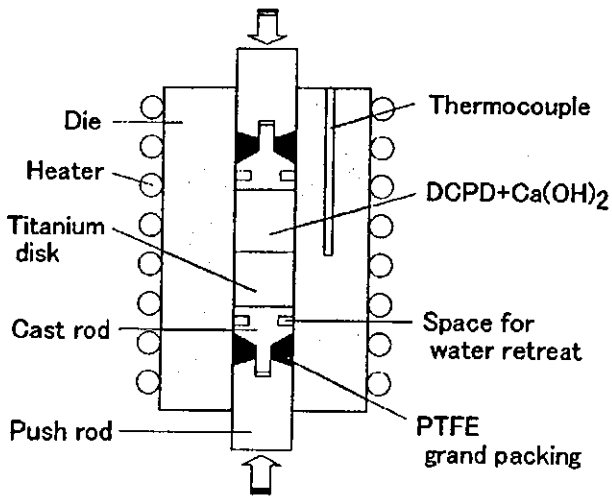

Fig. 1. Schematic illustration of the autoclave for hydrothermal hot-pressing (HHP).

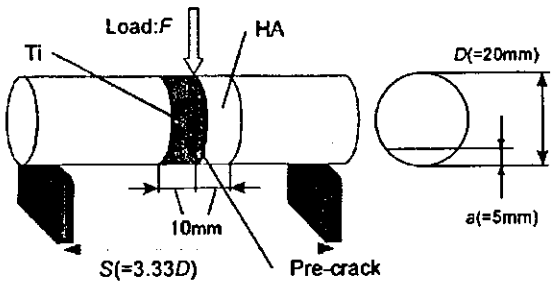

Fig. 2. Schematic illustration of the 3-point bending test.

HHP method. Core-based specimens were used for the fracture toughness tests following the ISRM suggested method [19]. The configuration of the core-based specimen is schematically shown in Fig. 2. In order to measure the interface toughness, stainless steel-rods were glued to the HA/Ti body and solidified HA body using epoxy resin in order to prepare standard core specimens specified in the ISRM suggested method. A pre-crack was introduced in the HA/Ti interface, as shown in Fig. 2. The depth and the width of the pre-crack were 5 mm and 50 μm, respectively. In order to determine the fracture toughness of the HA only, HA specimens were sandwiched and glued with stainless steel-rods. In this type of specimen, a pre-crack was introduced in the center of the HA ceramic.

The specimens were loaded at a cross-head speed of 1 mm/min until a fast fracture took place. The stress intensity factor K was employed to obtain an estimate of the fracture property of the HA/Ti interface and the HA ceramics, using the following equation:

$$K = 0.25(S/D) \cdot Y'_c \cdot (F/D^{1.5}) \quad (3)$$

where D is the diameter of the specimen (20 mm), S (=3.33D) is the supporting span, F is the load, Y'_c is the dimensionless stress intensity factor. The value of Y'_c can be found in the literature [19]. The critical stress intensity K_c was computed from the peak load at the onset of the fast fracture.

It should be mentioned here that the formula given in Eq. (3) is derived under the assumption of isotropic and homogeneous materials. The HA/Ti bonded specimen used in this study consists of two or three kinds of materials. While an exact anisotropic solution is needed for the quantitative evaluation of the stress intensity factor, the isotropic solution in Eq. (3) is used to obtain an estimate of the fracture toughness for the HA and HA/Ti specimens.

3. Results and discussion

A typical example of temperature and pressure records is shown in Fig. 3, along with volume ratio data. It is seen that the shrinkage started at approximately

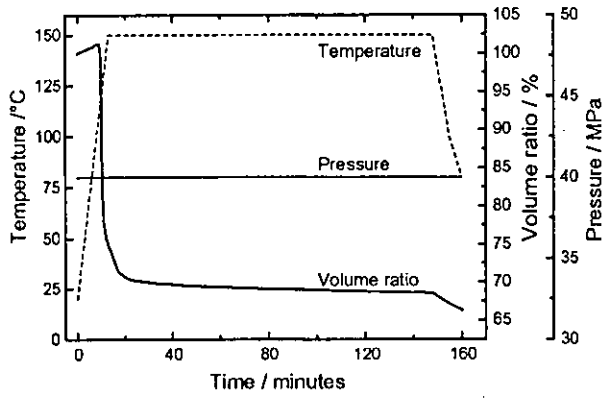

Fig. 3. Time variation of temperature, pressure and volume ratio during hydrothermal hot-pressing treatment.

90 °C. This temperature is close to the dehydration temperature of DCPD. Thus, it is thought that the shrinkage is initiated by the dehydration of DCPD. The shrinkage rate became larger with increasing temperature, and then the shrinkage rate became smaller. The shrinkage continued during the HHP treatment. The pressure was held at 40 MPa constant for the whole period of HHP treatment. As seen in Fig. 4, X-ray diffraction analysis showed that the DCPD and $Ca(OH)_2$ powder materials were completely transformed into HA by the HHP treatment. As demonstrated in Fig. 5, the HA ceramics could be bonded to the Ti disks at a low temperature of 150 °C using the above-mentioned HHP treatment. The density of the HA ceramics prepared by the HHP in this study was 1.9 Mgm^{-3}. In addition to the DCPD powder, three different types of powders were used as a starting material: HA and β-tri calcium phosphate (β-TCP). No bonding with a Ti disk was observed, when the above starting powders were used and treated by the HHP under the conditions of 150 °C and 40 MPa. Thus, DCPD was the only starting material that produced HA/Ti bonded bodies among the precursors for HA used in this study.

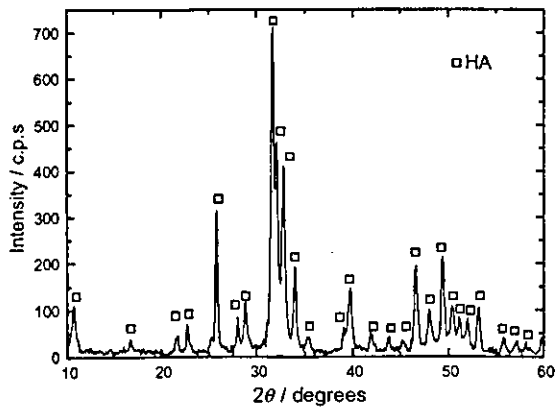

Fig. 4. X-ray diffraction pattern of the HA ceramics.

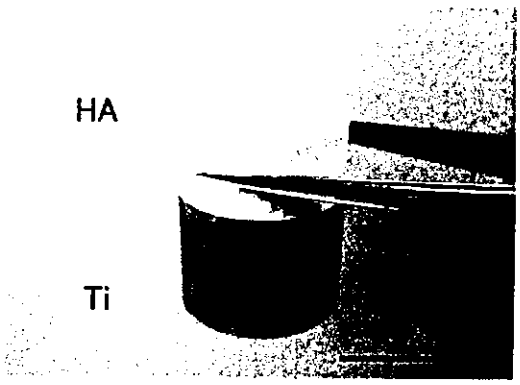

Fig. 5. Photograph of the bonded body of HA and Ti.

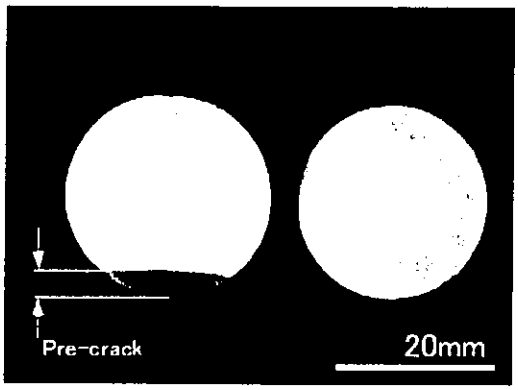

Fig. 6. Photograph of the fracture surface in a HA/Ti specimen after the 3-point bending test. Note that the crack propagated into the HA.

Fig. 6 shows a photograph of the fracture surface in the bonded HA/Ti body after the 3-point bending test. It can be noted that the crack initiated from the pre-crack tip and did not propagate along the HA/Ti interface, but into the HA. This observation suggests that the fracture toughness of the HA/Ti interface is close to or higher than that of the HA ceramics only. The critical stress intensity factor K_c was 0.30 MPa$m^{1/2}$ for the HA ceramics, and 0.25 MPa$m^{1/2}$ for the bonded HA/Ti. The toughness data are the average values obtained from at least five specimens. The K_c value for the bonded HA/Ti body gives a slightly lower value than that of the HA ceramics only. The difference in K_c data is potentially due to the residual stress induced by the thermal expansion mismatch between HA and Ti. The K_c value achieved for the pure Ti was close to the highest value obtained for the Ti alloys in our research [15]. The fracture appearance in Fig. 6 may suggest that the interface toughness should be equal to or higher than that of the HA ceramics only. While further development is needed to improve the fracture properties of the solidified HA, the HHP treatment may have the advantage over the plasma-spraying technique in the preparation of thermodynamically stable HA without decomposition. The above results demonstrate the usefulness of the HHP method for bonding HA and Ti in order to produce a bioactive layer in biomaterials.

4. Summary

In this paper, it was demonstrated that HA could be bonded to Ti using a hydrothermal hot-pressing method at a temperature as low as 150 °C with no special surface treatment of Ti. The fracture toughness tests conducted on the bonded HA/Ti body revealed that the crack propagation from the pre-crack tip did not occurre along the interface, but into the HA ceramics. The fracture toughness of the HA/Ti interface was also suggested to be close to or higher than that of the HA ceramics. Investigation of the bonding mechanism and in vivo tests of the HA/Ti bonded bodies are in progress.

Acknowledgement

This study was supported in part by the Japan Ministry of Health, Labour and Welfare under grants-in aid for Research on Advanced Medical Technology.

References

[1] Long M, Rack HJ. Biomaterials 1998;19:1621.
[2] Hench LL. J Am Ceram Soc 1998;81:1705.
[3] Jarcho M, Kay JF, Gummaer KI, Doremus RH, Drobeck HP. J Bioeng 1977;1:79.
[4] Aoki H. Medical applications of hydroxyapatite. Tokyo, Japan: Ishiyaku Euro-America; 1994. p. 133.
[5] Peelen JGJ, Rejda BV, De Groot K. Ceramurgia Int 1978;4:71.
[6] Hench LL. J Am Ceram Soc 1991;74:1487.
[7] Ducheyne P, Hench LL, Kagan A, Martens M, Burssens A, Mulier JC. J Biomed Mater Res 1980;14:225.
[8] Radin SR, Ducheyne P. J Mater Sci Mater Med 1992;3:33.
[9] De Groot K, Geesink R, Klein CPAT, Serekian P. J Biomed Mater Res 1987;21:1375.
[10] Zheng X, Huang M, Ding C. Biomaterials 2000;21:841.
[11] Gledhill HC, Turner IG, Doyle C. Biomaterials 2001;22:695.
[12] Fazan F, Marquis PM. J Mater Sci Mater Med 2000;11:787.
[13] Thomas KA. Orthopaedics 1994;17:267.
[14] Kokubo T, Kim H-M, Kawashita M. Biomaterials 2003;24:2161.
[15] Onoki T, Hosoi K, Hashida T. Key Eng Mater 2003;240–242:571.
[16] Yamasaki N, Yanagisawa K, Nishioka M, Kanahara S. J Mater Sci Lett 1986;5:355.
[17] Monma H, Kamiya T. J Mater Sci 1987;22:4247.
[18] Hosoi K, Hashida T, Takahashi H, Yamasaki N, Korenaga T. J Am Ceram Soc 1996;79:2771.
[19] Hashida T. Int J Rock Mech Min Sci Geomech Abstr 1993;30:61.

ELSEVIER

Biomaterials 23 (2002) 1091–1101

Biomaterials

www.elsevier.com/locate/biomaterials

Development of calcium phosphate cement using chitosan and citric acid for bone substitute materials

Atsuro Yokoyama[a,*], Satoru Yamamoto[a], Takao Kawasaki[a], Takao Kohgo[b], Masanori Nakasu[c]

[a] *Department of Removable Prosthetic Dentistry, School of Dentistry, Hokkaido University, North 13 West 7, Kika-ku, Sapporo, 060-8586, Japan*
[b] *Department of Oral Pathology, School of Dentistry, Hokkaido University, North 13 West 7, Kika-ku, Sapporo, 060-8586, Japan*
[c] *New Ceramics Department, Medical Instruments Division, Asahi Optical Co., Ltd. 2-36-9 Maeno-cho, Itabashi-ku, Tokyo, 174-8639, Japan*

Received 15 May 1999; accepted 11 June 2001

Abstract

We developed a calcium phosphate cement that could be molded into any desired shape due to its chewing-gum-like consistency after mixing. The powder component of the cement consists of α-tricalcium phosphate and tetracalcium phosphate, which were made by decomposition of hydroxyapatite ceramic blocks. The liquid component consists of citric acid, chitosan and glucose solution. In this study, we used 20% citric acid (group 20) and 45% citric acid (group 45). The mechanical properties and biocompatibility of this new cement were investigated. The setting times of cements were 5.5 min, in group 20 and 6.4 min, in group 45. When incubated in physiological saline, the cements were transformed to hydroxyapatite at 3, and 6 weeks, the compressive strengths were 15.6 and 20.7 MPa, in group 45 and group 20, respectively. The inflammatory response around the cement implanted on the bone and in the subcutaneous tissue in rats was more prominent in group 45 than in group 20 at 1 week after surgery. After 4 weeks, the inflammation disappeared and the cement had bound to bone in both groups. These results indicate that this new calcium phosphate cement is a suitable bone substitute material and that the concentration of citric acid in the liquid component affects its mechanical properties and biocompatibility.

Keywords: Calcium phosphate cement; Chitosan; Citric acid; Bone substitute material; Biocompatibility

1. Introduction

Hydroxyapatite (HAP) has been studied as a possible substitute material for hard tissue due to its high biocompatibility and osteoconductivity, and it has been used clinically as artificial bone and for dental implants [1,2]. However, the clinical use of HAP as a bone substitute has proved problematic. For example, it is difficult to prevent the dispersion of HAP granules and mold the granules into the desired shape [3]. On the other, when HAP is used in a block form, necrosis and perforation of the mucosa covering the blocks have been reported [4]. Efforts have been made in recent years to overcome these problems. Monma and Kanazawa reported that the hydration of α-tricalcium phosphate (α-TCP) occurred below 100°C in water and that the products were calcium-deficient HAP [5]. Brown and Chow reported on a calcium phosphate cement that consisted of tetracalcium phosphate (TeCP) and dicalcium phosphate dihydrate (DCPD) or dicalcium phosphate anhydrous (DCPA) [6]. It demonstrated good osteoconductivity [7,8] because it was finally transformed into HAP. Several studies have been performed on calcium phosphate cements [9–13]. Sumita a former colleague of ours, reported a self-hardening HAP that consisted of α-TCP and TeCP as the powder component and citric acid, chitosan and glucose solution as the liquid component. After mixing the powder and liquid components together, it showed chewing-gum-like consistency, and could be molded into the desired shape [14,15]. Mori reported that a prominent inflammatory response was seen around the material implanted in subcutaneous tissue in rats at 1 week after surgery [16]. We speculated that acid could cause the inflammatory response. The aim of the present study was to investigate the effect of the concentration of citric acid on the

*Corresponding author. Tel.: +81-11-706-4270; fax: +81-11-706-4903.
E-mail address: yokoyama@den.hokudai.ac.jp (A. Yokoyama).

0142-9612/02/$ - see front matter
PII: S0142-9612(01)00221-6

mechanical properties and biocompatibility, and develop a new calcium phosphate cement with improved mechanical properties and biocompatibility as a bone substitute.

2. Materials and methods

2.1. Materials

The cement developed in this study consisted of both powder and liquid components. The powder component was a mixture of α-TCP and TeCP at a molecular ratio of 2:1. The powder component was made by decomposition of a block of HAP (Apaceram^R, Asahi Optical Co. Ltd, Tokyo, Japan) for 1 hour at a temperature of 1200°C and a reduced pressure (10^{-2}–10^{-3} Pa). The molar Ca/P ratio of HAP (Apaceram^R) used in this study was 1.67. This reaction was according to the following equation:

$$Ca_{10}(PO_4)_6(OH)_2 \rightarrow 2Ca_3(PO_4)_2 + Ca_4(PO_4)_2O + H_2O.$$

The resulting mixture was uniform in composition. Details of the powder component were reported by Sumita [15]. XRD patterns of Apaceram^R (before decomposition) and the powder components are shown in Fig. 1. The liquid component was a solution of citric acid, chitosan (98% deacetylated) and glucose. In this study, two types of liquid components were used to investigate the effects of the concentration of citric acid on the mechanical properties and biocompatibility. One solution (group 45) contained citric acid (45% wt), glucose (15%) and chitosan (1%). The other solution (group 20) contained citric acid (20%), glucose (6.7%) and chitosan (1%). The powder/liquid ratio was 2.0 (wt/wt).

2.2. Setting times of the cements

Setting times of the cements were measured according to the international standard ISO 9917 for dental silicophosphate cement ($n = 5$).

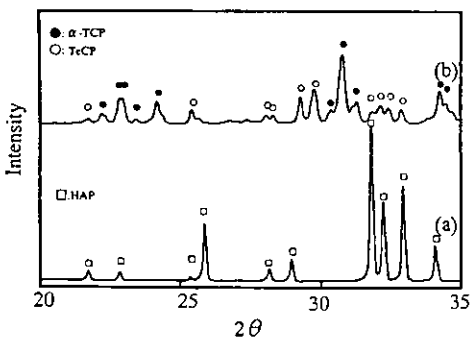

Fig. 1. X-ray diffraction patterns. (a) Apaceram^R (before decomposition) and (b) powder component.

2.3. Observation by SEM

After setting, the cements were observed under a scanning electron microscope (S-4000, Hitachi Co., Tokyo, Japan).

2.4. Mechanical strength

2.4.1. Compressive strength in an atmosphere of 100% humidity

Samples of each of the two types of cement were molded into columns (5.0 mm in diameter and 10.0 mm in length). The compressive strengths of the columns were measured using an Auto Graph (DSS 5000, Shimadzu, Tokyo, Japan) at a crosshead speed of 0.5 mm/min. Measurements were made at 1, 3, 5 and 10 days in an atmosphere at 37°C and 100% humidity ($n = 5$).

2.4.2. Compressive strength when incubated in physiological saline

Samples of each of the two types of cement were molded into columns (5.0 mm in diameter and 10.0 mm in length). After setting, the columns were immediately placed into physiological saline (100 ml) and incubated at 37°C. Compressive strengths were measured at 1, 3, 5 and 10 days and 3 and 6 weeks after incubation ($n = 5$). Physiological saline was changed every day.

2.5. Effects of glucose on the setting time and mechanical strength

Setting times and compressive strengths of the cements which contain glucose at various concentrations were measured to investigate the effects of glucose. Setting time was measured according to the ISO 9917. Compressive strengths were measured at 5 days after incubation. Physiological saline was not changed.

2.6. pH changes

Samples (A mixture of 2 g of powder and 1 g of liquid component) of each of the two types of cement were molded into columns that were then placed in physiological saline (50 ml) after setting. The pH values of physiological saline in which the samples were incubated at 37°C were measured at 5, 10, 20, 30, 60 and 120 min, at 1, 3, 5 and 10 days, and 2, 3, 4 and 6 weeks ($n = 3$). Physiological saline was changed every day.

2.7. Concentrations of Ca and P ions

Columns (5.0 mm in diameter and 10.0 mm in length) made from each of the two types of cement were incubated in physiological saline (100 ml) at 37°C. The

concentrations of Ca and P ions were measured at 1, 3, 5 and 10 days, and at 2, 3, 4 and 6 weeks after incubation. Concentrations of Ca and P ions were measured by emission spectro chemical analysis (ICPS-7500, Shimazu, Tokyo, Japan) ($n = 3$). Physiological saline was changed every day.

2.8. X-ray diffraction

The samples of the cements incubated in physiological saline for 1, 3, 5, 10 days, and for 2, 3, 4 and 6 weeks and the cements implanted in the subcutaneous tissue of rats for 2 and 4 weeks were analyzed by X-ray diffraction (PW1700, Philips Analytical X-ray B.V., Almelo, Netherlands). The intensities of some peaks, 29.8° (2θ) for TeCP, 30.8° (2θ) for α-TCP and 25.9° (2θ) for HAP were recorded and the amounts of transformation of the components of the cements into HAP on the cements incubated in physiological saline were estimated. The transformation rate was calculated by the following equation, modified from the report of Fukase et al. [17].

$$\text{Transformation rate}\,(\%) = 1/2[(P_{\text{HAP}(t)}/P_{\text{HAP}(\infty)}) + 2/3(1 - P_{\alpha\text{-TCP}(t)}/P_{\alpha\text{-TCP}(0)}) + 1/3(1 - P_{\text{TeCP}(t)}/P_{\text{TeCP}(0)})]\times 100,$$

where $P_{\alpha\text{-TCP}(0)}$ and $P_{\text{TeCP}(0)}$ are the intensities of the peaks of α-TCP and TeCP in the original powder components, respectively, and $P_{\text{HAP}(\infty)}$ is the intensity of the peaks of HAP in the cements at the point when the peaks TeCP and α-TCP were not detected (at 3 weeks in group 45 and 6 weeks in group 20 after incubation). $P_{\text{HAP}(t)}$, $P_{\alpha\text{-TCP}(t)}$ and $P_{\text{TeCP}(t)}$ are the intensities of peaks of HAP, α-TCP and TeCP, in the cement harvested at time t after incubation. Physiological saline was changed every day.

2.9. Biocompatibility

Eighteen 6-week old male Wistar rats were used in this study. The samples of the two types of cement were molded into pellets (4.5 mm in diameter and 1.5 mm in thickness). After hardening, the pellets were immediately implanted between the periosteum and parietal bone, and in the subcutanenous tissue of the thoractic region of rats. Rats were sacrificed at 1, 2 and 4 weeks after surgery and the tissue blocks containing the pellets were fixed in 10% neutral formalin, decalcified, and embedded in paraffin. Hematoxylin and eosin-stained specimens were observed by light microscopy. Animal experiments were done following the "Guide for the care and use of laboratory animals, School of Dentistry, Hokkaido University".

3. Results

3.1. Setting time

After mixing the powder and liquid components together, both types of cement (groups 20 and 45) had a "chewing-gum-like" consistency (Fig. 2) that could be molded into the desired shape. Setting times were 5.54 ± 0.15 min in group 20 and 6.40 ± 0.20 min in group 45 ($n = 5$).

3.2. Observation of SEM

As shown in Fig. 3a, SEM revealed the presence of numerous fine grains covering the surfaces of global structures approximately 10 μm in diameter in a sample from group 20. A sample from group 45 (Fig. 3b) showed global structures approximately 20 μm in a diameter on a smooth, platelike matrix.

3.3. Mechanical strength

Figs. 4 and 5 show the compressive strengths of the samples in an atmosphere of 100% humidity and in physiological saline, respectively. The compressive strength of samples from group 45 was significantly higher than that from group 20 at 100% humidity. However, while compressive strength constantly increased with time at 100% humidity in both groups, samples incubated in physiological saline showed an initial decrease in compressive strength at 3 days after incubation in group 20. Thereafter, the compressive strength increased with time. Whereas, the compressive strength of samples from group 45 was higher than that from group 20 during the initial 10 days in physiological saline, that of samples from group 20 at 6 weeks after

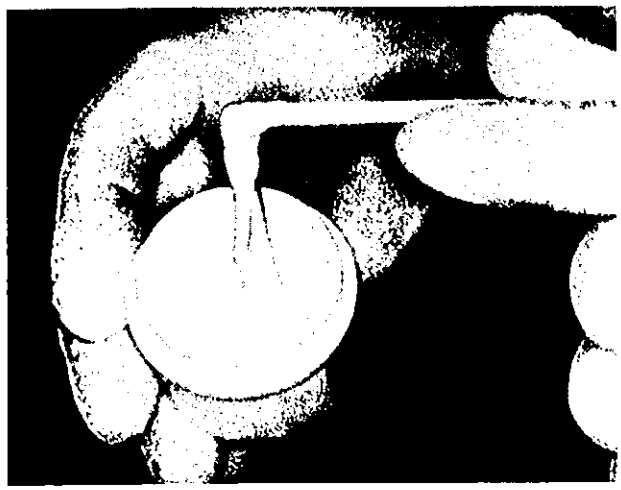

Fig. 2. The material showed chewing-gum-like consistency after mixing.

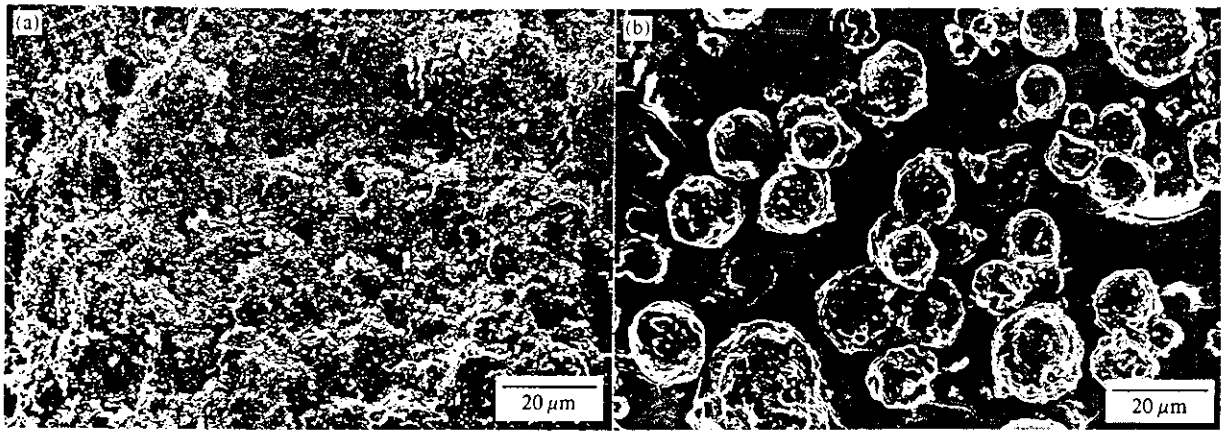

Fig. 3. Images of SEM: (a) group 20; and (b) group 45.

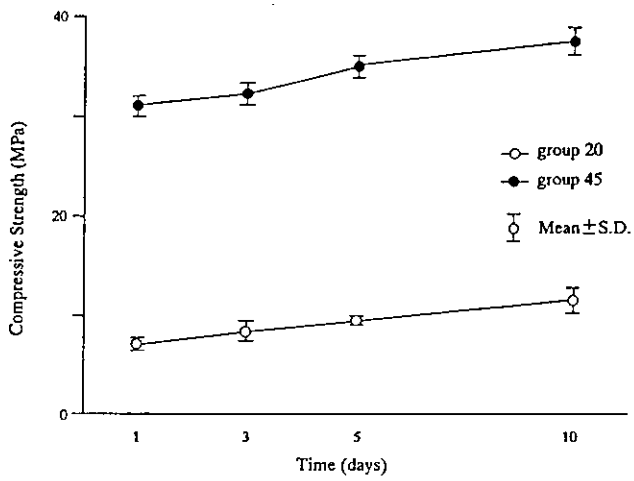

Fig. 4. Compressive strength in an atmosphere of 100% humidity.

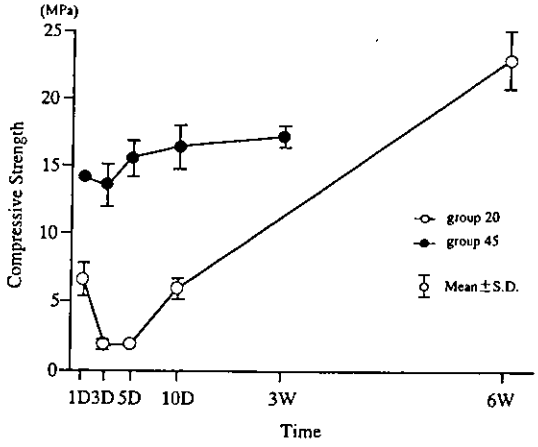

Fig. 5. Compressive strength when incubated in physiological saline.

incubation, which were transformed to HAP completely, was higher than that of samples from group 45 at 3 weeks after incubation, which were transformed to HAP completely.

3.4. Effects of glucose on setting time and compressive strength

Tables 1 and 2 show setting times and compressive strengths of the cements containing glucose at various concentrations. Setting time increased with the concentration of glucose in both cements. Compressive strength decreased when the concentration of glucose was increased in group 45, whereas the compressive strengths of the cements were almost the same regardless of the concentration of glucose in group 20.

3.5. Change in pH of physiological saline

The pH of the physiological saline in which the two types of cement were incubated increased with time in both groups (Figs. 6a and b). The pH of the saline in which group 20 samples were incubated was higher at each measurement point than that in which group 45 samples were incubated. The pH values were 6.70 ± 0.02 in group 20 and 5.98 ± 0.02 in group 45 at 120 min after the start of incubation. The pH values increased with incubation time and reached 7.04 at 5 days in group 20 and 6.94 at 3 days in group 45, when physiological saline was changed every day. After that, it gradually decreased with incubation time.

3.6. Concentrations of Ca and P ions

Figs. 7A and B show the concentrations of Ca and P ions in the physiological saline. The concentrations of Ca and P ions at 1 day after incubation were high, and those of group 45 were higher than those of group 20. Ca ions were detected at every measuring point and decreased with time in both cements, when physiological saline was changed every day. The concentration of Ca ions of group 45 was higher than that of group 20. P ions were hardly detected at 3 days after incubation and

Table 1
Effect of glucose on setting time

Group 20			Group 45		
Glucose	0%	4.76±0.09 min	Glucose	0%	1.88±0.10 min
	6.7%	5.54±0.15		5%	2.30±0.12
	10%	6.38±0.33		10%	3.43±0.14
	15%	7.60±0.27		15%	6.40±0.20
	20%	9.30±0.25		20%	8.27±0.25
				Mean±SD, $n = 5$	

Table 2
Effect of glucose on compressive strength

Group 20			Group 45		
Glucose	0%	3.07±0.28 MPa	Glucose	0%	50.62±10.52 MPa
	6.7%	4.07±0.45		5%	43.41±8.10
	10%	3.35±0.63		10%	20.47±2.69
	15%	3.71±0.32		15%	19.78±3.12
	20%	3.33±1.16		20%	21.65±4.02
				Mean±SD, $n = 5$	

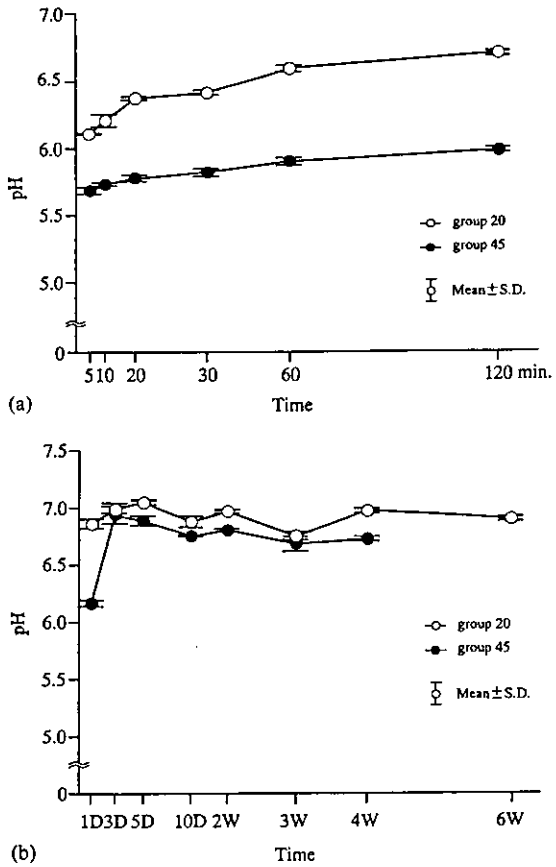

Fig. 6. The pH values of the physiological saline in which the samples were incubated.

increased gradually in group 20, but decreased with incubation time in group 45.

3.7. XRD analysis

Figs. 8(A) and (B) show the patterns of X-ray diffraction. Those of the powder components showed high α-TCP and TeCP peaks, and no HAP peak. Whereas, the peak of TeCP decreased from 1 day after incubation, the peaks of α-TCP did not change in group 20. From 10 days after incubation, the peaks of α-TCP began to decrease. The peaks of HAP became higher with incubation time, the peaks of TeCP and α-TCP were not detected at 6 weeks. On the other hand, the peaks of TeCP and α-TCP decreased from 1 day, the peaks of HAP became higher and the peaks of TeCP and α-TCP were not detected at 3 weeks in group 45. The transformation to HAP in vitro was faster than that in vivo. Fig. 9 shows the changes of the rates of transformation to HAP. The rates increased with incubation time in both cements, and that of group 45 was higher than that of group 20.

3.8. Biocompatibility

3.8.1. Soft tissue response

In the granulation tissue, numerous dilated capillaries, mesenchymal cells and thin collagen fibers were observed around the implanted cement at 1 week after

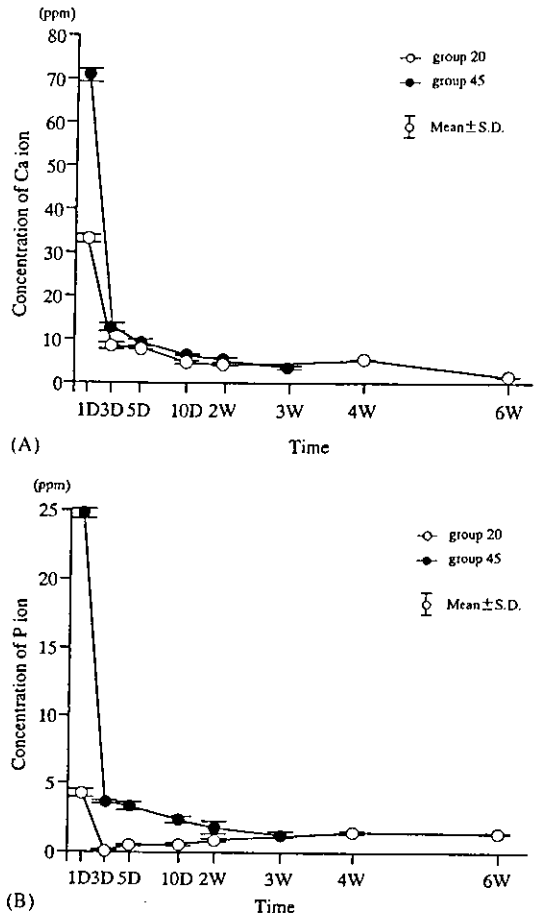

Fig. 7. (A) Concentrations of Ca ions in the physiological saline solutions in which the samples were incubated; (B) concentrations of P ions in the physiological saline in which the samples were incubated.

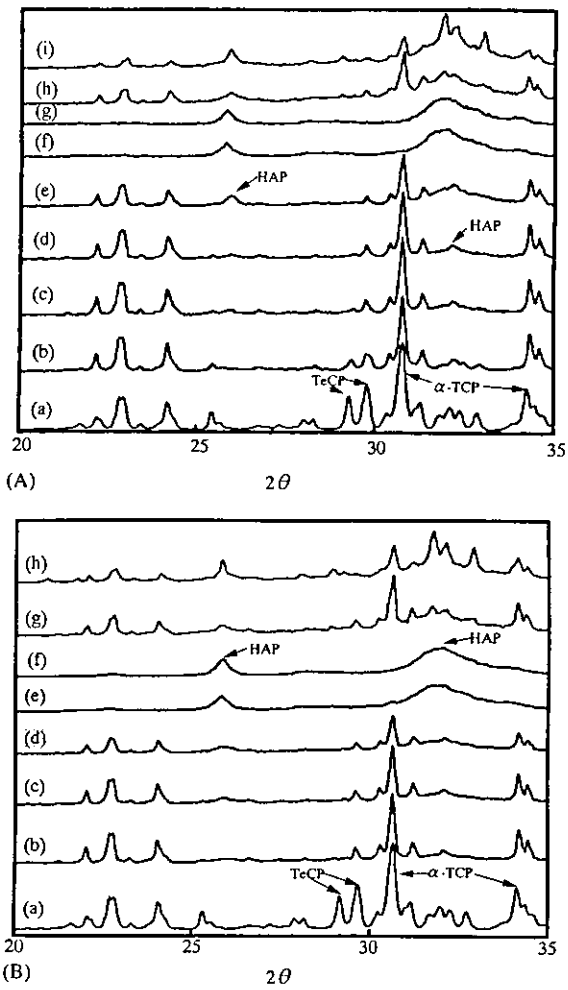

Fig. 8. (A). X-ray diffraction patterns of group 20: (a) powder component; (b) at 1 day after incubation in physiological saline; (c) at 3 days after incubation in physiological saline; (d) at 5 days after incubation in physiological saline; (e) at 10 days after incubation in physiological saline; (f) at 4 weeks after incubation in physiological saline; (g) at 6 weeks after incubation in physiological saline; (h) at 2 weeks after implantation in subcutaneous tissue; and (i) at 4 weeks after implantation in subcutaneous tissue. (B): X-ray diffraction patterns of group 45: (a) powder component; (b) at 1 day after incubation in physiological saline; (c) at 3 days after incubation in physiological saline; (d) at 5 days after incubation in physiological saline; (e) at 10 days after incubation in physiological saline; (f) at 3 weeks after incubation in physiological saline; (g) at 2 weeks after implantation in subcutaneous tissue; and (h) at 4 weeks after implantation in subcutaneous tissue.

surgery. In group 45, hyalinization was observed on the surfaces of the implanted cement. Foreign body giant cells were observed on the surface of the cements in both groups, although they were more numerous in group 45 than in group 20. Inflammatory cell infiltration was more prominent in the granulation tissue in group 45 (Fig. 10b) than in group 20 (Fig. 10a). With time, inflammatory responses around the implanted cements gradually decreased in both groups and the implanted cements were covered by layers of dense collagen fibers. Few inflammatory round cells and foreign body giant cells were observed at 4 weeks after surgery (Figs. 11a and b).

3.8.2. *Hard tissue response*

At 1 week after surgery, numerous dilated capillaries, mesenchymal cells and slight inflammatory cell infiltration were seen in the thickened periosteum that covered the implanted cement in group 20 (Fig. 12a). In group 45, hyaline degeneration and moderate inflammatory cell infiltration were seen in the prominent hypertrophic periosteum (Fig. 12c). On the surface of the parietal bone around the cement, granulation tissue with mesenchymal cells and capillaries and newly formed bone from the parietal bone (not bound to the cement) were observed in group 20 (Fig. 12b), but no new bone formation was seen in group 45 (Fig. 12d). At 2 weeks after surgery, an inflammatory response around the cement was still present in group 45, but in group 20 inflammation had disappeared and newly formed bone was seen to be partially bound to the cement. At 4 weeks after surgery, the inflammatory response disappeared in group 45 and newly formed bone from the parietal bone was seen to be partially bound to the cement (Figs. 13c

and d). Many parts of the surface of the grafted material in group 20 that was bound to the newly formed bone showed lamella-like structures and bone marrow space formation (Figs. 13a and b).

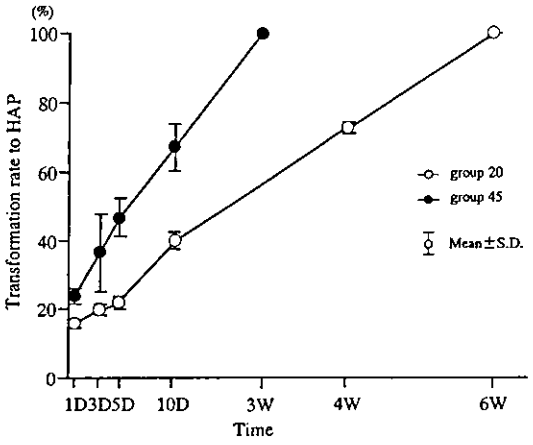

Fig. 9. Rate of transformation to HAP.

4. Discussion

Although sintered HA ceramics have good biocompatibility and osteoconductivity, they lack sufficient plasticity for easy molding into the desired shape. The newly developed cement reported in this study has excellent handling properties and moldability. Unlike the calcium phosphate cements that have been reported previously, this material had chewing-gum-like consistency after mixing, as shown in Fig. 2. Thus, this material could be molded to fit the shape of even the most complicated bone defect and would be useful in oral and plastic surgery. This chewing-gum-like consistency is thought to be due to the addition of chitosan to the liquid component. Chitosan is a polysaccharide, a partially deacetylated chitin (98% deacetylated chitin was used in this study), which has high viscosity in solution [18], and which has recently been widely used as a biomaterial because of its biocompatibility [19,20]. Cherng reported that the incorporation of chitosan acetate and chitosan lactate could improve the handling

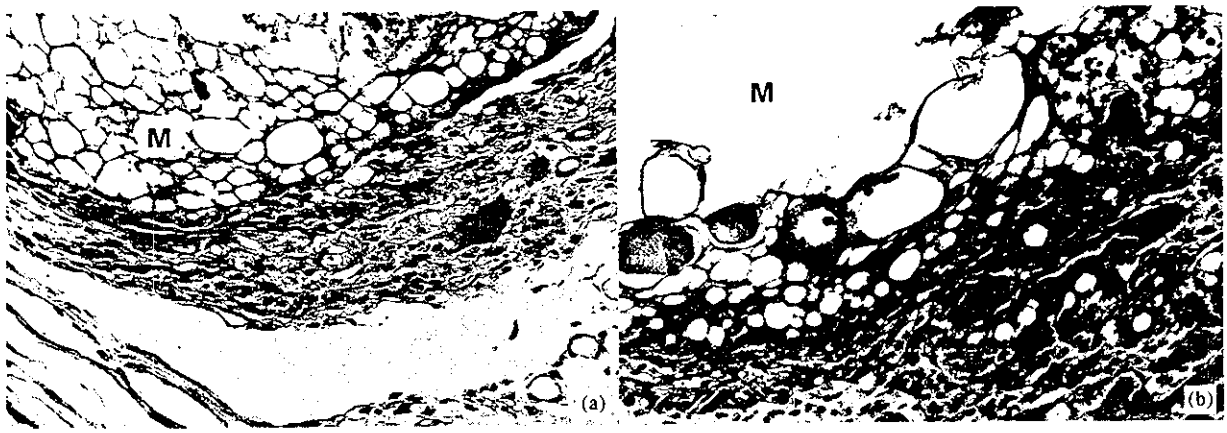

Fig. 10. Light micrographs of tissue responses around materials at 1 week after implantation in subcutaneous tissue: (a) group 20; and (b) group 45; (M) grafted material. Inflammatory cell infiltration is more prominent in group 45 than in group 20. Original magnification × 100.

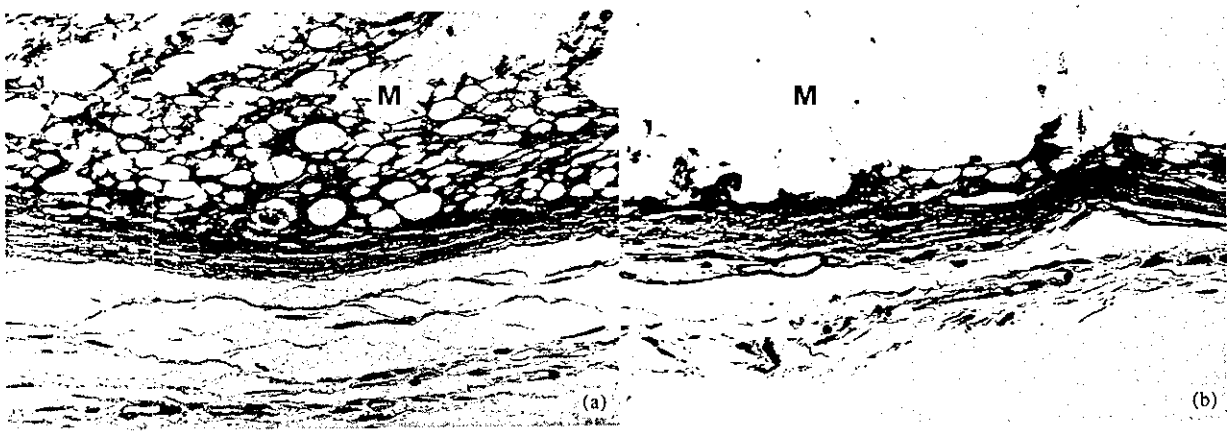

Fig. 11. Light micrographs of tissue responses around materials at 4 weeks after implantation in subcutaneous tissue: (a) group 20; and (b) group 45; (M) grafted material. The grafted materials are covered by dense collagen fibers in both groups. Original magnification × 100.

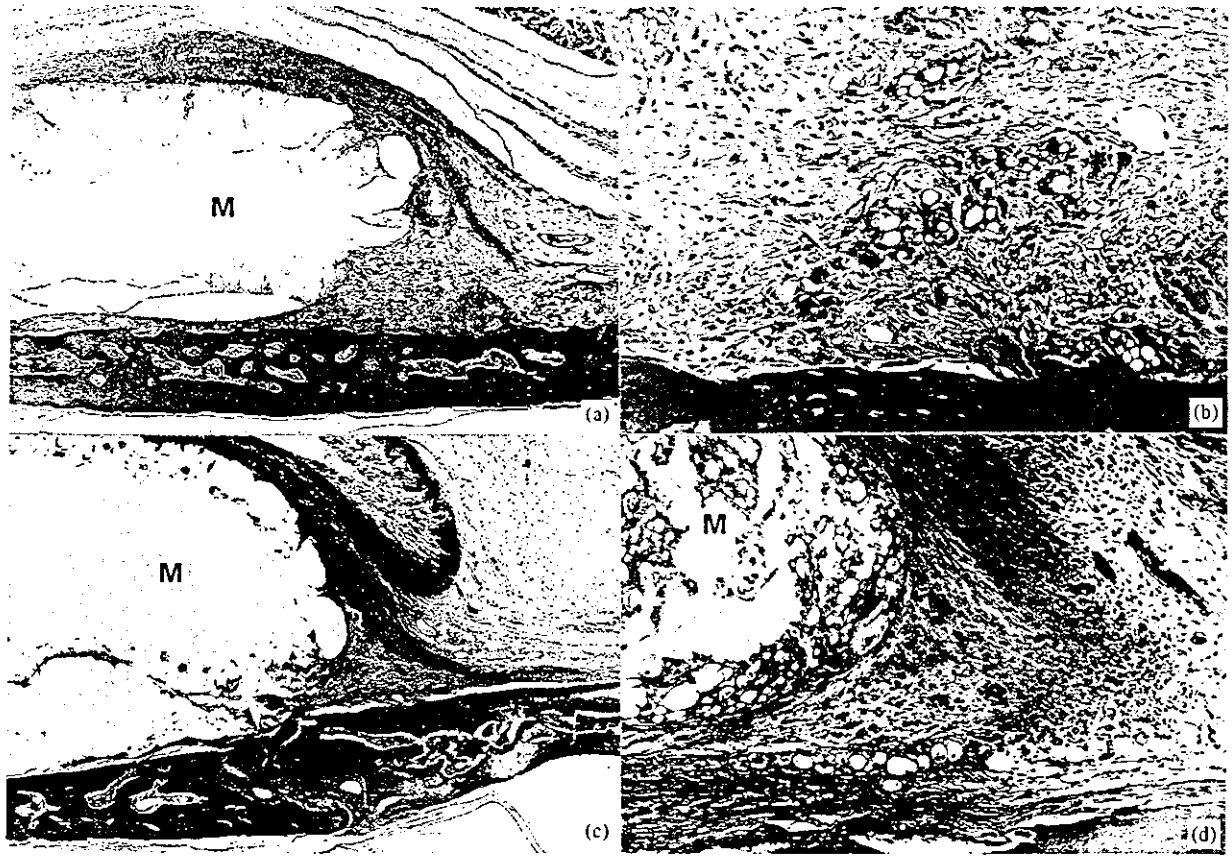

Fig. 12. Light micrographs of tissue responses around materials at 1 week after implantation between periosteum and parietal bone: (a) group 20. Thickened periosteum with slight inflammatory cell infiltration can be seen. Original magnification × 10; (b) group 20. Newly formed bone from the parietal bone can be seen. Original magnification × 50; (c) group 45. Prominent hypertrophic periosteum can be seen. Original magnification × 10; (d) group 45. Moderate inflammatory cell infiltration can be seen around the grafted material. No new bone formation can be seen × 50; (M) grafted material.

properties of calcium phosphate cement [21]. Takechi that reported anti-washout calcium phosphate cement containing chitosan showed excellent biocompatibility [22].

The results from the present study demonstrated that the concentration of citric acid influenced kinetics, mechanical properties and biocompatibility of the cements. The setting reactions of the cements could be divided into two stages. The initial hardening was a chelate reaction between citric acid in the liquid component and calcium in the powder component and the second reaction was transformation of the components of the cements to HAP. It has been reported that calcium phosphate cement containing carboxylic acid hardens rapidly, with a poor soluble matrix by chelation [22,23]. In our experiment, it appeared that the compressive strength at the early stage was affected by the degree of chelation. Therefore, the difference between the compressive strengths of groups 20 and 45 during the initial 10 days after incubation can be explained as a difference in the degree of chelation due to variations in the concentration of citric acid. The transformation of the components of the cements to HAP also appeared to be influenced by the concentration of citric acid. The XRD analysis of group 20 showed that the peak of TeCP decreased, and the peak of α-TCP did not decrease during the initial 5 days after incubation in saline. These results demonstrated that only TeCP was dissolved and transformed to HAP. TeCP was transformed according to the following equation [24].

$$3Ca_4(PO_4)_2O + 3H_2O \rightarrow Ca_{10}(PO_4)_6(OH)_2 + 2Ca(OH)_2. \quad (1)$$

The increase of pH by 5 days after incubation in spite of the change of the saline solution every day was due to the dissolution and transformation of TeCP. The lack of detection of P ions at 3 day suggested that P ions released by dissolution of TeCP were used for the formation of HAP. The decrease of the peak of α-TCP from day 10 suggested that α-TCP was dissolved and transformed to HAP. α-TCP was transformed according

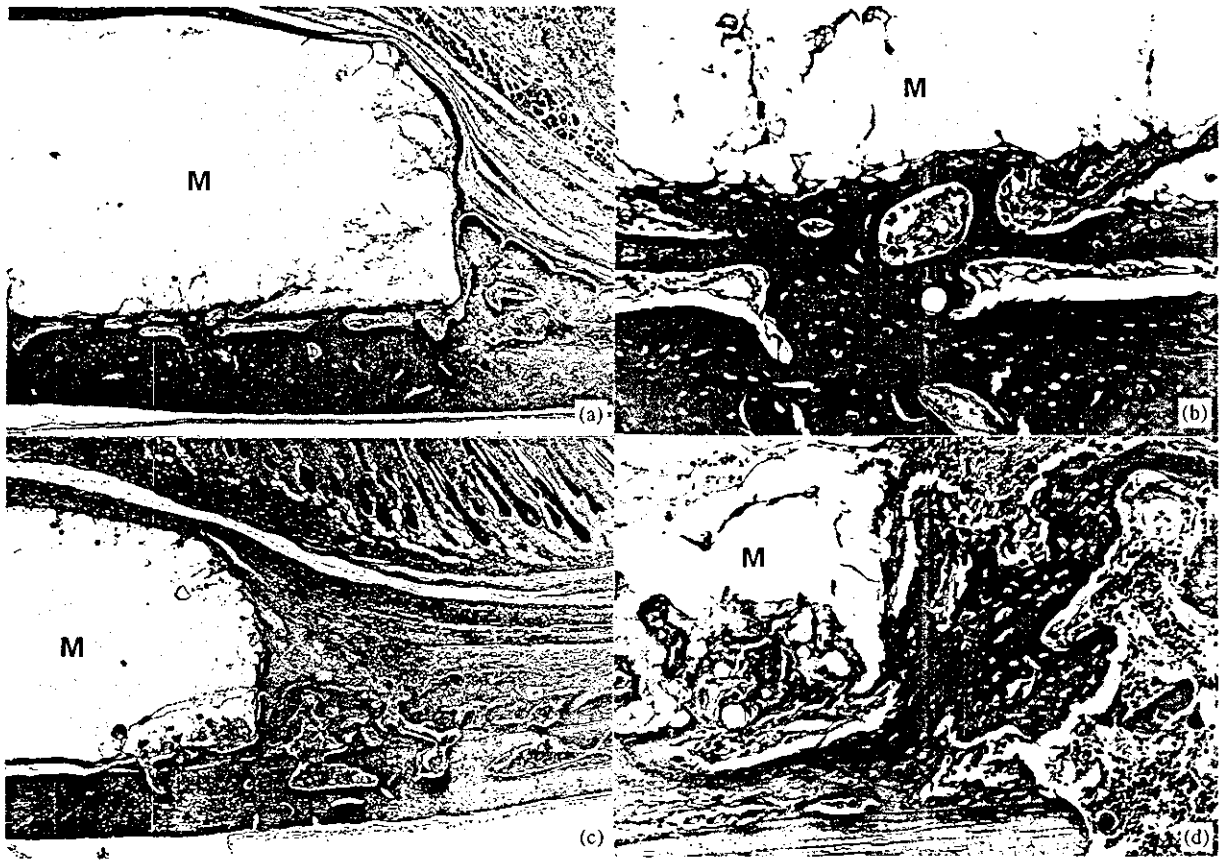

Fig. 13. Light micrographs of tissue responses around materials at 4 weeks after implantation between periosteum and parietal bone: (a) group 20. Many parts of the surface of the material are directly bound to the newly formed bone. Original magnification × 10; (b) group 20. Lamella-like structures and bone marrow can be observed in the newly formed bone. Original magnification × 50; (c) group 45. Newly formed bone is partially bound to the material. Original magnification × 10; (d) group 45. Immature waven bone can be seen to be bound to the material × 50; (M) grafted material.

to the following equation [25]:

$$10Ca_3(PO_4)_2 + 6H_2O \rightarrow 3Ca_{10}(PO_4)_6(OH)_2 + 2H_3PO_4. \quad (2)$$

Some reports on calcium phosphate cement containing α-TCP have demonstrated that α-TCP reacts to calcium-deficient HAP [12,13]. The increase of P we observed was hypothesized to be related to the progress of this reaction when the saline was changed every day. After 4 weeks, the peak of TeCP was hardly detected. Therefore, it was presumed that Eq. (2) progressed dominantly after 4 weeks. On the other, in group 45, the decrease of the peaks of both TeCP and α-TCP, which meant dissolution and transformation, occurred simultaneously from 1 day after incubation, although the decrease of α-TCP was less than that of TeCP. Concentrations of P ions at 3, 5 and 10 days were higher than those of group 20, and decreased with time in contrast to group 20. These results suggested that the reaction shown in Eq. (2) was generated dominantly in the early incubation stage in group 45. Since transformation of α-TCP occurred faster than in group 20, the rate of transformation to HAP of group 45 was higher than that of group 20. Therefore, the compressive strength of group 45 by day 10 was higher than that of group 20. Ginebra et al. reported that the compressive strength of calcium phosphate cement was related to the extent of the hydrolysis of α-TCP [13]. In our study, the compressive strength of group 45 increased from 1 day, while that of group 20 increased from 10 days when transformation of α-TCP occurred. The decrease of the compressive strength of group 20 at 3 days after incubation can be explained by the dissolution of TeCP and the slight formation of HAP. The decrease of the compressive strength occurred by the dissolution of TeCP from the cement was supposed to be more than the increase of that occurred by the transformation of TeCP to HAP. The compressive strength of group 20, which was completely transformed to HAP, was higher than that of group 45 completely transformed to HAP. This inversion of compressive strength may indicate dissolution of calcium citrate, which was a chelate reaction product. The quantity of calcium citrate seems

to be related to the difference of kinetics between group 20 and group 45. Monma reported that carboxylic ions accelerate hydration of α-TCP [23]. Therefore, transformation to HAP of group 45 appeared to be faster than that of group 20. The compressive strength at 100% humidity was higher than that after incubation in physiological saline. It is thought that interlocking of HAP crystals was inhibited in physiological saline, as reported by Ishikawa et al. [11]. The setting time was shorter in group 20 than in the group 45 in spite of its higher concentration of citric acid. This was due to the effect of glucose in the liquid component. Tables 1 and 2 show that glucose influenced the setting times and compressive strengths of the cements. In particular, group 45, which contained a high concentration of citric acid, was more strongly affected by glucose than group 20, so glucose was hypothesized to inhibit the effect of citric acid.

Analysis by XRD was carried out on the cements implanted in subcutaneous tissue. The degree of transformation to HAP in vivo at 4 weeks after implantation into rat subcutaneous tissue was lower than that in vitro at 4 weeks after incubation in physiological saline, as shown in Figs. 8A and B. The material implanted in the subcutaneous tissue was surrounded by fibrous tissue in the organization process; thus, this material had less chance to come into contact with body fluids such as blood.

When using an organic acid in liquid component of the cement, it is necessary to consider the inflammatory response induced by the acid in the early implantation stage. The pH value was lower in group 45 than in group 20. The presence of surplus acid would cause an inflammatory response in vivo. Kurashina et al. reported that α-TCP hardened by the addition of acid was surrounded by fibrous tissue and did not bind directly to bone in rabbits [26]. They speculated that the acid caused the formation of the fibrous capsules. In the present study, a moderate inflammatory response was seen in the subcutaneous tissue and around the bone soon after the implantation of samples from group 45. However, only a slight inflammatory response was seen in the subcutaneous tissue and around the bone after the implantation of samples from group 20. Thus, the concentration of citric acid affected the biocompatibility of the cement in soft tissue and bone. At 4 weeks after implantation, there was only a slight inflammatory response in the subcutaneous tissue and the cement had bound directly to the bone even in group 45. These results are similar to those reported by Kurashina [27] for implants on the parietal bone in rabbits and Miyamoto [28] for implants in the tibia in rats. For cement samples implanted between the periosteum and bone, the surplus acid is buffered by bleeding. Thus, the inflammatory response induced by the acid is less than that for samples implanted in subcutaneous tissue. Furthermore, although the samples were implanted immediately after setting, there were no cases of the cement being broken, dissolved, or washed out into the tissue. For this reason, it is thought that an insoluble matrix was formed through chelation. No resorption of either cement was observed in the subcutaneous tissue or between the periosteum and parietal bone within 4 weeks. Several studies have reported the resorption and replacement of calcium phosphate cement [26–30]. In our study, the duration of the experiment was too short to investigate the resorption of the cement. Thus, further experiments are necessary to investigate it.

5. Conclusion

We developed a new calcium phosphate cement that consists of chitosan, glucose and citric acid solution as the liquid component, and α-TCP and TeCP as the powder components. This cement could be molded to desired shape because of its chewing-gum-like consistency after mixing, and it demonstrated good biocompatibility in both soft and hard tissues. In this study, liquid components of 20% and 45% citric acid were used to investigate the influence of acid, and the results indicated that the concentration of citric acid in the liquid component influences both the mechanical properties and biocompatibility of the cement.

References

[1] Kent JN, Finger IM, Quinn JH, Guerra LR. Hydroxyapatite alveolar ridge reconstraction: clinical experience, complications and technical modifications. J Oral Maxilofac Surg 1986; 44:37–49.
[2] Kent JN, Block MS, Finger IM, Guerra L, Larsen H, Misiek DJ. Biointegrated hydroxyapatite coated dental implants: 5-year clinical observations. J Am Dent Assoc 1990;121:138–44.
[3] Wittkampf ARM. Augmentation of the maxillary alveolar ridge with hydroxylapatite and fibrin glue. J Oral Maxillofac Surg 1988;46:1019–21.
[4] Hupp JR, Mckenna S. Use of porous hydroxylapatite blocks for augmentation of atrophic mandibles. J Oral Maxillofac Surg 1988;46:538–45.
[5] Monma H, Kanazawa T. The hydration of α-tricalcium phosphate. Yogyo-Kyokai-shi 1976;84:209–13.
[6] Brown WE, Chow LC. Combinations of sparingly soluble calcium phosphates in slurries and paste as mineralizers and cements. US Patent 4,612,053, 1986.
[7] Hong YC, Wang JT, Hong CY, Brown WE, Chow LC. The periapical tissue reactions to a calcium phosphate cement in the teeth of monkeys. J Biomed Mater Res 1991;25:485–98.
[8] Sugawara A, Nishiyama M, Kusama K, Moro I, Nishinura S, Kudo I, Chow LC, Takagi S. Histolpathological reactions of calcium phosphate cement. Dent Mater J 1992;11:11–6.
[9] Bermudez O, Botlong MG, Driessens FCM, Planell JA. Development of some calcium phosphate cements from

combinations α-TCP, MCPM and CaO. J Mater Sci: Mater Med 1994;5:160–3.
[10] Ishikawa K, Takagi S, Chow LC, Ishikawa Y. Properties and mechanisms of fast-setting calcium phosphate cements. J Mater Sci: Mater Med 1995;6:528–33.
[11] Ishikawa K, Miyamoto Y, Kon M, Nagayama M, Asaoka K. Non-decay type fast-setting calcium phosphate cement: composite with sodium alginate. Biomaterials 1995;16:527–32.
[12] Fernandez E, Ginebra MP, Boltong MG, Driessens FCM, Ginebra J, De Maeyer EAP, Verbeeck RMH, Planell JA. Kinetic study of the setting reaction of a calcium phosphate bone cement. J Biomed Mater Res 1996;32:367–74.
[13] Ginebra MP, Fernandez E, De Maeyer EAP, Verbeeck RMH, Boltong MG, Ginebra J, Driessens FCM, Planell JA. Setting reaction and hardening of an apatitic calcium phosphate cement. J Dent Res 1997;76:905–12.
[14] Sumita M. Development of chitosan/calcium phosphate composite material for bone substitute materials. Kino Zairyo 1989; 9:26–32 (in Japanese).
[15] Sumita M. Composition for forming calcium phosphate type setting material and process for producing setting materials US Patent, 5,281,404, 1994.
[16] Mori K, Ohno K, Kudo M, Michi K, Shigeno K, Hirayama Y. Histological study of self-setting apatite bone substitute—comparative study of hardening materials and non hardening materials. J Jpn Stomatol Soc 1993;42:695–703.
[17] Fukase Y, Eanes ED, Takagi S, Chow LC, Brown WE. Setting reactions and compressive strengths of calcium phosphate cements. J Dent Res 1990;69:1852–6.
[18] Mita Y. Properties of chitosan and use for material of cosmetics. In: Food Chemical. I. Tokyo: Shokuhin-Kagaku-Shinbunsha, 1987; 70–78 (in Japanese).
[19] Muzzarelli R, Baldassarre V, Conti F, Ferrara P, Biagini G, Gazzanelli G, Vasi V. Biological activity of chitosan: ultrastructural study. Biomaterials 1988;9:247–52.
[20] Muzzarelli RA, Biagini G, Bellardini L, Simonelli L, Castaldini C, Fratto G. Osteoconduction exerted by methylpyrrolidinone chitosan used in dental surgery. Biomaterials 1993;14:39–43.
[21] Cherng A, Takagi S, Chow LC. Effects of hydroxypropyl methylcellulose and other gelling agents on the handling properties of calcium phosphate cement. J Biomed Mater Res 1997;35:273–7.
[22] Takechi M, Miyamoto Y, Ishikawa K, Toh T, Yuasa T, Nagayama M, Suzuki K. Initial histological evaluation of anti-washout type fast-setting calcium phosphate cement following subcutaneous implantation. Biomaterials 1998; 19:2057–63.
[23] Monma H. Materials chemistry of calcium phosphate cement. J Jpn Soc Biomater 1997;15:24–30.
[24] Ishikawa K, Kuwayama N, Tagagi S, Chow LC. The development of fast-setting calcium phosphate cement. Jpn J Dent Mater 1993;12:222–3.
[25] Monma H, Goto M, Kohmura T. Effect of additives on hydration and hardening of tricalcium phosphate. Gypsum Lime 1984; 188:11–6.
[26] Kurashina K, Ogiso A, Kotani A, Takeuchi H, Hirano M. Histological and microradiographic evaluation of hydrated and hardened α-tricalcium phosphate/calcium phosphate dibasic mixtures. Biomaterials 1994;15:429–32.
[27] Kurashina K, Kurita H, Kotani A, Kobayashi S, Kyoshima K, Hirano M. Experimental cranioplasty and skeltal augmentation using an α-tricalcium phosphate/dicalcium phosphate dibasic/tetracalcium phosphate monoxide cement: preliminary short-term experiment in rabbits. Biomaterials 1998;19:701–6.
[28] Miyamoto Y, Ishikawa K, Takeuchi M, Toh T, Yoshida Y, Nagayama M, Kon M, Asaoka K. Tissue response to fast-setting calcium phosphate cement in bone. J Biomed Mater Res 1997;37:457–64.
[29] Friedman CD, Costantino PD, Jones K, Chow LC, Pelzer HJ, Sisson GA. Hydroxyapatite cement. II. Obliteration and reconstruction of the cat frontal sinus. Arch Otolaryngo Head Neck Surg 1991;117:385–9.
[30] Shindo ML, Costantino PD, Friedman CD, Chow LC. Facial skeletal augmentation using hydroxyapatite cement. Arch Otolaryngo Head Neck Surg 1993;119:185–90.

Tissue response to a newly developed calcium phosphate cement containing succinic acid and carboxymethyl-chitin

Atsuro Yokoyama,[1] Hironobu Matsuno,[1] Satoru Yamamoto,[1] Takao Kawasaki,[1] Takao Kohgo,[2] Motohiro Uo,[3] Fumio Watari,[3] Masanori Nakasu[4]

[1]*Department of Oral Functional Science, Hokkaido University Graduate School of Dental Medicine, Kita13 Nishi7 Kita-ku, Sapporo 060-8586, Japan*

[2]*Department of Oral Pathobiological Science, Hokkaido University Graduate School of Dental Medicine, Kita13 Nishi7 Kita-ku, Sapporo 060-8586, Japan*

[3]*Department of Oral Health Science, Hokkaido University Graduate School of Dental Medicine, Kita13 Nishi7 Kita-ku, Sapporo 060-8586, Japan*

[4]*New Ceramics Department, Asahi Optial Co., Ltd. 2-36-9, Maeno-cho, Itabashi-ku, Tokyo 174-8639, Japan*

Received 23 April 2001; revised 15 April 2002; accepted 25 April 2002
Published online 30 January 2003 in Wiley InterScience (www.interscience.wiley.com). DOI: 10.1002/jbm.a.10398

Abstract: We developed a new calcium phosphate cement containing succinic acid and carboxymethyl-chitin in the liquid component. In this study, the biocompatibility and osteoconductivity of this new cement were investigated. After mixing, cement in putty form was implanted immediately between the periosteum and parietal bone and in the subcutaneous tissues of rats. In control cement, distilled water was used instead of the liquid component. In addition to histological evaluations, analyses with X-ray diffraction and Fourier transform infrared were performed for the subcutaneously implanted cements. Histological examination showed slight inflammation around the new cement on the bone and in the subcutaneous tissue at 1 week after surgery. At 2 weeks, the cement was partially bound to the parietal bone. The extent of the surface of the new cement directly in contact with the bone increased with time, and most of the undersurface of the new cement bound to the host parietal bone by 8 weeks. Analysis by X-ray diffraction showed that the new cement in the subcutaneous tissue was transformed into hydroxyapatite by 8 weeks. These results indicate that this new calcium phosphate cement is useful as a bone substitute material. © 2003 Wiley Periodicals, Inc. J Biomed Mater Res 64A: 491–501, 2003

Key words: calcium phosphate cement; succinic acid; CM-chitin; biocompatibility; osteoconductivity

INTRODUCTION

Hydroxyapatite (HAP) has been used as a bone substitute material because of its high biocompatibility and osteoconductivity.[1,2] The HAP ceramics that are currently used clinically lack sufficient plasticity and thus cannot be molded easily into the desired shapes to fit complicated surgical sites. Therefore, complications such as the perforation of the mucosa covering HAP used in block form and the dispersion of HAP used in granule form have been reported.[3,4] Monma and Kanazawa reported that the hydration of α-tricalcium phosphate occurs below 100°C in water and that the product is calcium-deficient HAP.[5] In 1986 Brown and Chow developed a calcium phosphate cement that consisted of tetracalcium phosphate and dicalcium phosphate anhydrous or dicalcium phosphate dihydrate[6] that had good osteoconductivity.[7] After their report, several studies were performed on calcium phosphate cements.[8–13] Constantz et al. reported the clinical use of calcium phosphate cement for skeletal repair.[12] We added carboxylic acid and polysaccharide as components of calcium phosphate cement to improve its mechanical and handling properties. We previously reported on calcium phosphate cement containing citric acid as a carboxylic acid and chitosan as a polysaccharide.[14] It could be easily molded into the desired shape because of its chewing gum-like consistency after mixing and it demonstrated good osteoconductivity but provoked a moderate inflammatory response around the cement in the early implantation stage. To improve the inflammatory response, we developed a new calcium phosphate cement containing succinic acid as a carboxylic acid and carboxymethyl-chitin (CM-chitin) as a polysaccharide.

Correspondence to: A. Yokoyama; e-mail: yokoyama@den.hokudai.ac.jp

It had putty-like consistency after mixing and thus could be molded into any desired shape.[15] The prehardened form of cement implanted in the subcutaneous tissue caused a slight inflammatory response, and there was a moderate inflammatory response when the cement was implanted in the putty form. Because it seemed that the inflammatory response was related to the acid content, we reduced the content of succinic acid from 8% to 3.9%. Although the setting time was increased from 7.3 min. to 14.2 min. by reducing the content of succinic acid, the compressive strength was almost the same. When soaked in the phosphate-buffered saline (PBS), this improved cement was transformed to HAP at 3 weeks. Furthermore, it did not break, even when soaked in distilled water immediately after mixing.[16,17] For clinical use, calcium phosphate cement should be used in putty form rather than in prehardened form when the handling properties are considered. We investigated the tissue response, especially osteogenesis, around the new calcium phosphate cement implanted in the putty form in this study.

MATERIALS AND METHODS

Calcium phosphate cement

This cement consisted of powder components and liquid components. The powder component consisted of a mixture of alpha-tricalcium phosphate (α-TCP), tetracalcium phosphate (TeCP), and dicalcium phosphate dihydrate (DCPD) at a molecular ratio of 2:1:3. The liquid component consisted of 4.0 wt % CM-chitin, 3.9 wt % succinic acid, and 4.4 wt % disodium hydrogen phosphate solution. The powder/liquid ratio used in this study was 2.3. As a control cement, the powder component was used with the distilled water instead of the liquid component. The setting times of the cements were 14.2 ± 0.57 min, in this new cement and 32.1 ± 0.69 min, in the control cement. When incubated in PBS, the compressive strengths at 1 week were 33.1 ± 3.04 and 23.7 ± 1.96 Mpa, and transformation rates to HAP at 2 weeks were 93.5 ± 0.97 and 81.6 ± 2.8% for the new cement and the control cement, respectively. Finally, this new cement was completely transformed to HAP at 3 weeks and the control cement was transformed after 4 weeks in PBS. The kinetics and mechanical properties of this new cement and the control cement have been reported in detail.[16,17]

Animal experiments

Fifty-one male 6-week-old Wistar rats were used in this study. Twenty-eight rats received the new cement and twenty-three rats received the control cement. Under general anesthesia, incisions were made bilaterally in the thoracic region and in the forehead. Two pockets were made in the subcutaneous tissue and one pocket on the parietal bone where the periosteum was detached from the cranium. After mixing the powder and liquid components and molding the cement into pellets (approximately 5 mm in diameter and 2 mm in thickness) by using a 1-cm^3 plastic syringe (Fig. 1), the cements were implanted in putty form. One pellet was implanted on the parietal bone and two pellets were implanted in the subcutaneous tissue in the thoracic region bilaterally in each rat. Calcein (CA), alizarine complexone (AC), and oxytetracycline hydrochloride (TC) were injected into the peritoneal cavity as hard-tissue labels. Rats used for analyses with X-ray diffraction (XRD) and Fourier-transform infrared spectroscopy (FT-IR) received the pellets only in subcutaneous tissue. The control cement was implanted as in the new cement group. Animal experiments were performed in accordance with the *Guide for the Care and Use of Laboratory Animals*, Hokkaido University Graduate School of Dental Medicine. During the course of the study, no rats were lost.

Histological evaluation

Three rats each were sacrificed for the histological evaluation of the new cement group at 1, 2, 4, 8, 16, and 52 weeks. For the control cement group, three rats each were sacrificed for histological evaluation at 2, 4 and 26 weeks and two rats were sacrificed each at 1 and 8 weeks. A total of 18 rats were used for histological evaluation of the new cement and 13 rats for that of the control cement. Tissue blocks from the parietal bone containing cement were fixed and divided into two parts sagittaly with a dental diamond disc under physiological saline flow for cooling. One of the two tissue blocks was used as a decalcified specimen and the other as an undecalcified specimen. Likewise, one specimen of the two cements implanted in the subcutaneous tissue of each rat was used as a decalcified specimen and the other was used as an undecalcified specimen. The tissue blocks for decalcified specimens were decalcified and embedded in paraffin. Hematoxylin and eosin-stained specimens were observed by light microscopy. The tissue blocks for undecalcified speci-

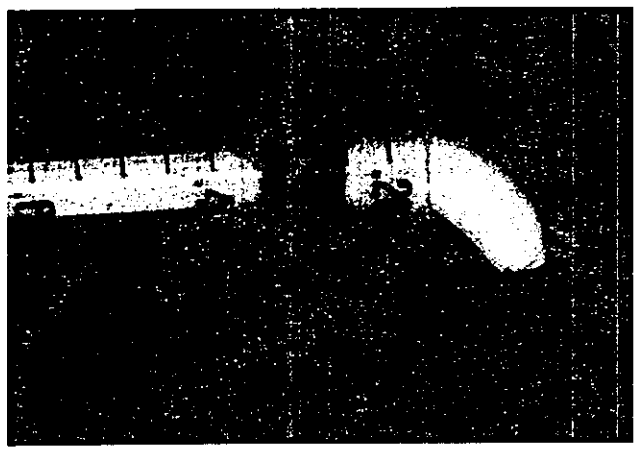

Figure 1. New cement shows putty-like consistency after mixing.

mens were stained with Villanueva bone stain, dehydrated, and embedded in polymethyl methacrylate resin. Thin, undecalcified specimens were observed by light microscopy and fluorescent microscopy.

The specimens were examined for tissue reactions such as inflammation and osteogenesis around the implanted cements. The inflammation was evaluated by the degree of the appearance of macrophages, foreign body giant cells, and the dilatation of capillaries. Osteogenesis around the cements was evaluated histologically by the degree of direct contact between the cement and the newly formed bone.

XRD and FT-IR analysis

Twenty rats were used for the analyses by XRD and FT-IR analysis. Two rats each were sacrificed at day 1 and 1, 2, 4, and 8 weeks for the new and control cement groups. The harvested cement was freeze-dried and divided into two parts. One part was used for XRD analysis and the other was for FTIR analysis. Therefore, four specimens were analyzed at the above-mentioned times for XRD and FTIR.

XRD spectra were measured by the powder diffraction method. The materials were scanned from 20.00 to 40.00° in 2θ. Then the intensities of some peaks, 23.4° (2θ) for DCPD, 29.8° (2θ) for TeCP, 30.8°(2θ) for α-TCP, and 25.9°(2θ) for HAP, were recorded and the amount of transformation of the components of the cement into HAP was estimated. The transformation rate was calculated by the following equation, modified from the report by Fukase et al.[18]

$$\text{Transformation rate (\%)} = 1/2[(P_{HAP(t)}/P_{HAP(\infty)}) + 3/6(1 - P_{DCPD(t)}/P_{DCPD(0)}) + 2/6(1 - P_{\alpha-TCP(t)}/P_{\alpha-TCP(0)}) + 1/6(1 - P_{TeCP(t)}/P_{TeCP(0)})] \times 100$$

$P_{DCPD(0)}$, $P_{\alpha-TCP(0)}$, and $P_{TeCP(0)}$ are the intensities of the peaks of DCPD, α – TCP, and TeCP in the original powder components, $P_{HAP(\infty)}$ is the intensity of the peak of HAP in the final product (3 weeks soaked in PBS). $P_{HAP(t)}$, $P_{DCPD(t)}$, $P_{\alpha-TCP(t)}$, and $P_{TeCP(t)}$ are the intensities of peaks of HAP, DCPD, α – TCP, and TeCP, respectively, in the cement harvested at time t after surgery.

FT-IR was used to investigate the chelates in the cement. After being ground into powder, the materials were mixed with a 9-fold volume of KBr powder. The infrared spectra between 2000 cm^{-1} and 500 cm^{-1} were measured by diffuse-reflectance spectroscopy. As the control material for detection of the chelates, calcium succinate was also measured.

RESULTS

Soft tissue response

New cement group

At 1 week after surgery, the cement was covered by granulation tissue with slight inflammatory changes. Some foreign body giant cells were seen on the surface of the cement [Fig. 2(a,b)]. CA injected at surgery was deposited on the surface of the cement and diffuse deposition of TC injected at 2 weeks after surgery was observed on the inner layer of the cement at 2 weeks [Fig. 2(c)]. At 4 weeks after surgery, the cement was covered by thin connective tissue with fibroblasts. In the lateralmost layers of the cement, mesh-like structures stained by hematoxylin were observed [Fig. 2(d)]. There were few foreign body giant cells on the surface of the cement, Cell-mediated distinct absorption of the cement was not observed at 52 weeks [Fig. 2(e)].

Control cement group

At 1 week after surgery, the cement was broken into particles and covered by granulation tissue with moderate inflammatory changes. We observed many foreign body giant cells, macrophages, and dilatation of capillaries. In addition, a small number of lymphocytes and plasma cells were observed sporadically in the granulation tissue. Numerous foreign body giant cells were seen on the surface of the cement [Fig. 3(a,b)]. Although CA was deposited on the cement, the extent of the deposited area was smaller and weaker than that of the new cement [Fig. 3(c)]. At 4 weeks after surgery, many foreign body giant cells were observed around the crumbled cement, whereas the moderate inflammatory changes decreased [Fig. 3(d,e)]. At 26 weeks, the cement was covered by thin fibrous connective tissue [Fig. 3(f)].

Hard tissue response

New cement group

At 1 week after surgery, the new cement was covered by granulation tissue with slight inflammatory changes. New bone formation from preexisting cortical bone was seen around the edge of the cement, but it was not bound to the cement. At 2 weeks, extensive new bone formation was seen in the gap between the host parietal bone and the cement. Newly formed bone bound to part of the cement directly [Fig. 4(a)]. Thin new bone was observed on part of the undersurface of the cement detached from the host parietal bone at 4 weeks [Fig. 4(b)]. New bone grew with time, and most of the edge and undersurface of the cement directly contacted the newly formed bone at 8 weeks [Fig. 4(c)]. CA injected at surgery was observed on the lateralmost layer of the cement, whereas AC, injected at 8 weeks, was distributed on the inner part of the CA layer [Fig. 4(d)]. Although most of the upper surface of the cement was covered by thin connective tissue, slight bone formation was observed on the upper sur-

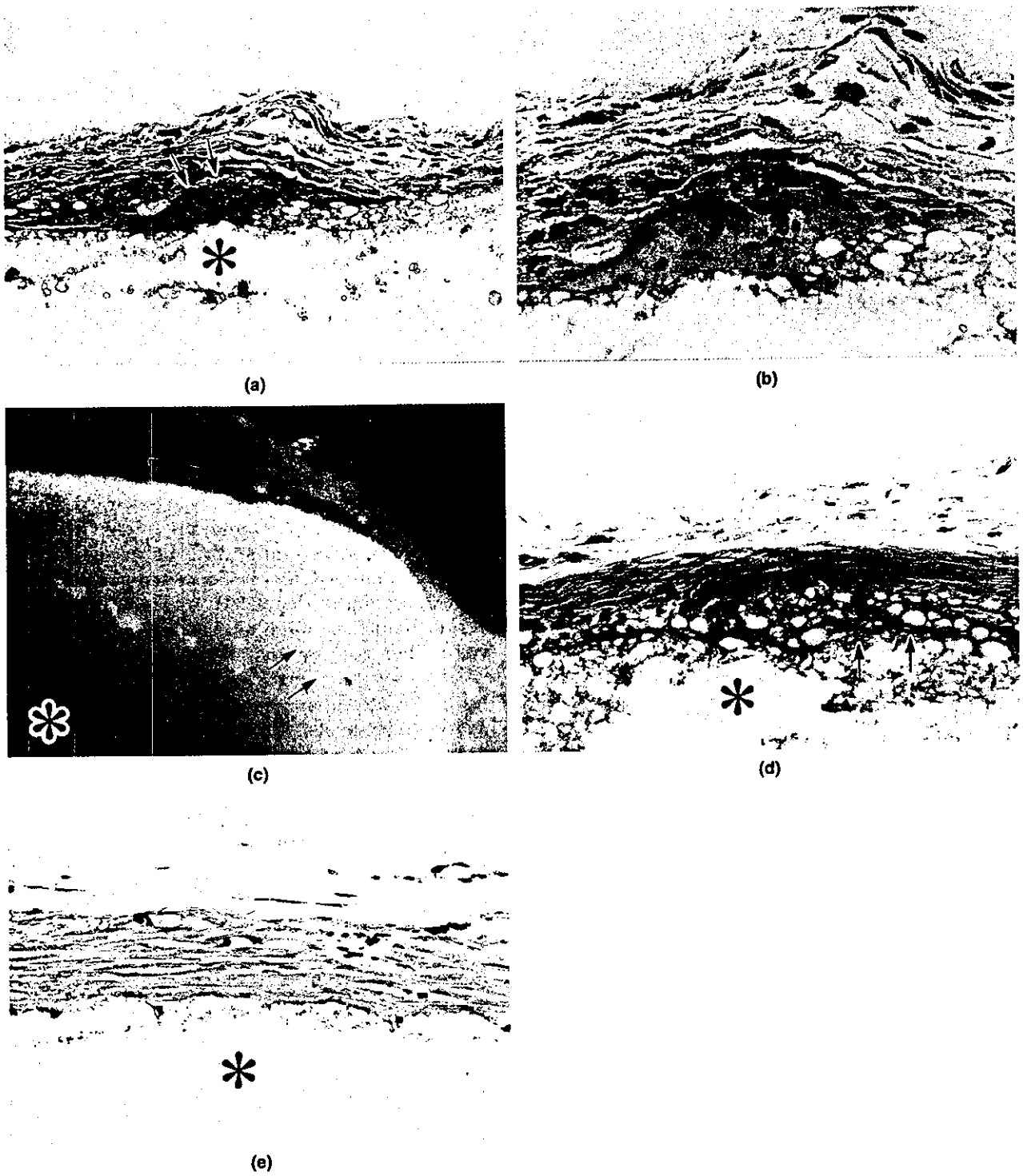

Figure 2. Soft tissue response to the new cement. (a) Slight inflammation and foreign body giant cell (arrow) are seen on the new cement (*) at 1 week after surgery. Hematoxylin and eosin stain: original magnification ×100. (b) High magnification of (a). Foreign body giant cell is seen on the surface of the new cement. Some mesenchymal cells and fibroblasts are seen in the granulation tissue around the new cement. Hematoxylin and eosin stain: original magnification ×200. (c) Calcein (arrowhead) injected at surgery is deposited on the surface of the new cement and oxytetracycline hydrochloride (arrow), injected at 2 weeks is observed on the inner layer of the cement (*) at 2 weeks after surgery. Fluorescent microscopy: original magnification ×25. (d) Cement (*) is covered by thin connective tissue, and a mesh-like structure (arrow) stained by hematoxylin was observed in the lateralmost layer of the cement at 4 weeks. Hematoxylin and eosin stain: original magnification ×100. (e) No foreign body giant cell can be observed on the surface of the cement (*) at 52 weeks. Hematoxylin and eosin stain: original magnification ×100.